

Article

# Effects of Immobilizations of rhBMP-2 and/or rhPDGF-BB on Titanium Implant Surfaces on Osseointegration and Bone Regeneration

So-Hyoun Lee <sup>1,†</sup>, Eun-Bin Bae <sup>1,†</sup>, Sung-Eun Kim <sup>2,†</sup>, Young-Pil Yun <sup>2</sup>, Hak-Jun Kim <sup>2</sup>, Jae-Won Choi <sup>1</sup>, Jin-Ju Lee <sup>1</sup> and Jung-Bo Huh <sup>1,\*</sup>

<sup>1</sup> Department of Prosthodontics, Dental Research Institute, Institute of Translational Dental Sciences, BK21 PLUS Project, School of Dentistry, Pusan National University, 49 Pusan University-Ro, Yangsan-Si 50612, Gyeongsangnam-Do, Korea; romilove7@hanmail.net (S.-H.L.); 0228dmqls@hanmail.net (E.-B.B.); won9180@hanmail.net (J.-W.C.); lju1112@hanmail.net (J.-J.L.)

<sup>2</sup> Department of Orthopedic Surgery and Rare Diseases Institute, Korea University Medical College, Guro Hospital, #80, Guro-dong, Guro-gu, Seoul 08308, Korea; sekim10@korea.ac.kr (S.-E.K.); ofeel0479@korea.ac.kr (Y.-P.Y.); dakjul@korea.ac.kr (H.-J.K.)

\* Correspondence: huhjb@pusan.ac.kr; Tel.: +82-10-8007-9099

† These authors contributed equally to this work.

Received: 23 November 2017; Accepted: 30 December 2017; Published: 31 December 2017

**Abstract:** The aim of this study was to examine the effects of immobilizing rhPDGF-BB plus rhBMP-2 on heparinized-Ti implants on in vivo osseointegration and vertical bone regeneration at alveolar ridges. Successful immobilizations of rhPDGF-BB and/or rhBMP-2 onto heparinized-Ti (Hepa/Ti) were confirmed by in vitro analysis, and both growth factors were found to be sustained release. To evaluate bone regeneration, rhPDGF-BB, and/or rhBMP-2-immobilized Hepa/Ti implants were inserted into beagle dogs; implant stability quotients (ISQ), bone mineral densities, bone volumes, osseointegration, and bone formation were assessed by micro CT and histometrically. In vivo study showed that the osseointegration and bone formation were greater in the rhPDGF-BB/rhBMP-2-immobilized Hepa/Ti group than in the rhPDGF-BB-immobilized Hepa/Ti group. The rhPDGF-BB/rhBMP-2 immobilized Hepa/Ti group also showed better implant stability and greater bone volume around defect areas and intra-thread bone density (ITBD) than the rhBMP-2-immobilized Hepa/Ti group. However, no significant differences were observed between these two groups. Through these results, we conclude rhBMP-2 immobilized, heparin-grafted implants appear to offer a suitable delivery system that enhances new bone formation in defect areas around implants. However, we failed to observe the synergetic effects for the rhBMP-2 and rhPDGF-BB combination.

**Keywords:** rhBMP-2; rhPDGF-BB; heparin; implant surface; osseointegration; bone regeneration; beagle dog

## 1. Introduction

Dental implants have been generally used as credible and secure treatments for the restoration of function and aesthetics of edentulous patients [1]. However, patients who have insufficient bone quality and quantity, or poor healing and regenerative capacities have been reported to experience unfavorable results after implant treatment [2]. To improve the success rate of these patients, it is important to increase the initial fixation of implant fixtures and to shorten the time required for the upper prosthesis to connect [3]. Recently, developments have focused on biomimetic treatment techniques based on applying biomolecules, such as bone morphogenetic protein (BMP) or platelet-derived growth factor (PDGF), to implant surfaces to address these problems [4–6].

BMP is a well-known growth factor that enhances bone regeneration by inducing the differentiation of mesenchymal stem cells to osteoblasts and promotes biosynthesis of bone matrix by regulating factors that are required for osteoinduction [7,8]. BMP-2, which is one of the 16 members of the BMP family, has been proven to be used in a variety of medical treatments by animal and clinical studies [4]. In particular, in one study an anodized titanium implant coated with recombinant human BMP-2 (rhBMP-2) produced by genetic recombination was found to be an effective carrier of rhBMP-2 [5]. However, several studies have reported that rhBMP-2 has no significant effect on bone formation [9,10]. These negative results were suggested to be due to large initial release of rhBMP-2, lack of standardization of the optimal rhBMP-2 concentration, and the use of only one type of growth factor, as natural regeneration process in man involves multiple growth factors [11–14].

Platelet-derived growth factor (PDGF), which is well-characterized tissue growth factor has been used in numerous *in vivo* and clinical studies [15–20], and has been shown to effectively promote bone, ligament, and cement regeneration in the periodontology field. [21,22]. PDGF is present in bone matrix and is secreted from platelets locally at fracture sites during initial fracture repair [23,24]. PDGF-BB is one of the five PDGF isoforms and is biologically the most potent and binds with greatest affinity to osteoblasts [6,25]. PDGF-BB has both mitogenic and chemotactic effects on osteoblasts and stimulates collagen I synthesis by osteoblasts [23]. It is also important for embryologic skeletal development, and when used topically, it can accelerate fracture healing in animals [26]. PDGF-BB has also been efficaciously used to treat osteoporosis in rodents, in which it improved trabecular bone strength and density [27].

Heparin is a natural linear polysaccharide and a highly sulfated glycosaminoglycan that binds strongly with various growth factors [28]. Biomaterial systems containing heparin exhibit controlled growth factor release [29,30]. When heparin was covalently grafted on anchored free amino positive groups on titanium surfaces, the primary amine groups of growth factors, such as BMP-2 or PDGF-BB, were found to bind to the carboxyl groups of bound heparin [31]. In a previous study, we suggested PDGF-BB/Hepa-Ti system exhibited promising potentials for the enhancements the functions of osteoblast [32]. Also in another previous study on PDGF-BB and BMP-2 co-delivery system on Hep-Ti substrates, the co-delivery system positively promoted functions of osteoblasts [6]. Many experiments have been performed on heparin and growth factor combinations in attempts to induce proper growth factor release, but these experiments were performed at the cellular level or under conditions too far removed from clinical situations.

Therefore, the purpose of this study was to confirm the effects of rhPDGF-BB and rhBMP-2 co-delivery in large animals using clinically reproducible conditions. rhPDGF-BB or/and rhBMP-2 were immobilized onto the surfaces of heparinized-Ti implants and inserted into open defects in beagle dog models. Histomorphometric analysis was conducted to evaluate the effect of rhPDGF-BB, rhBMP-2, and rhPDGF-BB/rhBMP-2 implants on osseointegration and bone regeneration.

## 2. Materials and Methods

### 2.1. Materials

Titanium discs (diameter 1.2 cm; height 0.3 cm) were supplied by Cowellmedi (Busan, Korea). Recombinant human platelet-derived growth factor-BB (rhPDGF-BB), recombinant human bone morphogenic protein-2 (rhBMP-2), rhPDGF-BB, and rhBMP-2 ELISA kits were purchased from PeproTech Inc. (Rocky Hill, NJ, USA). Ascorbic acid, dexamethasone,  $\beta$ -glycerophosphate, and dopamine were from Sigma-Aldrich (St. Louis, MO, USA), and heparin sodium (molecular weight: 12,000–15,000 g/mol) was from Acrose Organics (Belgium, NJ, USA). Dulbecco's modified Eagle's medium (DMEM), fetal bovine serum (FBS), phosphate-buffered saline (PBS), and penicillin-streptomycin (PS) were from Gibco BRL (Rockville, MD, USA).

## 2.2. Surface Modification of Titanium (Ti) with Heparin-Dopamine (Hepa-DOPA) and rhPDGF-BB and/or rhBMP-2

In order to immobilize rhPDGF-BB and/or rhBMP-2, Ti surfaces were modified with heparin-dopamine (Hepa-DOPA). Ti discs were placed in 10 mL Tris-HCl buffer (pH 8.0, 10 mM) containing 2 mg/mL Hepa-DOPA in the darkroom for 24 h. The Hepa-DOPA modified Ti disc was rinsed with distilled water (DW) and dried under nitrogen. Hepa-DOPA modified Ti is hereafter referred to as Heparinized-Ti (Hepa/Ti). To immobilize both rhPDGF-BB and rhBMP-2 on the surface of Hepa/Ti, a Hepa/Ti disc was immersed in MES buffer solution (pH 5.6, 0.1 M), and then rhPDGF-BB (50 ng/mL) and rhBMP-2 (50 ng/mL) were added. The reaction was allowed to proceed for 24 h at room temperature (RT), and then the disc was rinsed with DW and dried. rhPDGF-BB and rhBMP-2 immobilized on Hepa/Ti disc are hereafter referred to as PDGF/BMP/Hepa/Ti disc. rhPDGF-BB (100 ng/mL) or rhBMP-2 (100 ng/mL) modified Hepa/Ti disc were also fabricated using the same method. rhPDGF-BB or rhBMP-2 immobilized on Hepa/Ti disc are hereafter referred to as PDGF/Hepa/Ti or BMP/Hepa/Ti disc, respectively.

## 2.3. Characterization of Ti, Hepa/Ti, PDGF/Hepa/Ti, BMP/Hepa/Ti, and PDGF/BMP/Hepa/Ti Substrates

### 2.3.1. Scanning Electron Microscope (SEM) Image

The surfaces of Ti, Hepa/Ti, PDGF/Hepa/Ti, BMP/Hepa/Ti, and PDGF/BMP/Hepa/Ti disc were observed by scanning electron microscopy (SEM; S-2300, Hitachi, Tokyo, Japan). Samples were coated with gold using a sputter coater (Eiko IB, Eiko Engineering, Tokyo, Japan) and SEM was performed at 3 kV.

### 2.3.2. X-ray Photoelectron Spectroscopy (XPS)

The surface chemical compositions of Ti, Hepa/Ti, PDGF/Hepa/Ti, BMP/Hepa/Ti, and PDGF/BMP/Hepa/Ti disc were investigated by X-ray photoelectron spectroscopy (XPS; K-Alpha spectrometer; Thermo Electron, Rockford, IL, USA). Amounts of heparin immobilized onto Ti were measured using toluidine blue. Hepa/Ti disc was immersed in 1 mL PBS buffer (pH 7.4) containing 1 mL 0.005% toluidine blue, gently shaken for 30 min, and 2 mL of hexane was added. After removing the disc, absorbance of the aqueous phase was measured by a Flash Multimode Reader (Varioskan™, Thermo Scientific, Waltham, MA, USA) at 620 nm. The amount of heparin immobilized onto disc were calculated using a calibration curve prepared using different concentrations of heparin.

### 2.3.3. In Vitro rhPDGF-BB and rhBMP-2 Release

To determine the releases of rhPDGF-BB and rhBMP-2 from PDGF/Hepa/Ti, BMP/Hepa/Ti, and PDGF/BMP/Hepa/Ti, a prepared disc was placed in a 15 mL conical tube (Falcon, North Haledon, NJ, USA) containing PBS buffer (pH 7.4) at 37 °C with 100 rpm. At predetermined times of 1 h, 3, 6, and 10 h, and 1, 3, 5, 7, 10, 14, 21, and 28 days, supernatants were collected and buffer was replenished with an equal volume of fresh PBS. Amounts of rhPDGF-BB and rhBMP-2 released were determined using an enzyme-linked immunosorbent assay kit (ELISA), according to the manufacturer's instruction using a Varioskan Flash Multimode Reader (Thermo Fisher Scientific, Waltham, MA, USA) at 450 nm.

## 2.4. In Vitro Cell Study

### 2.4.1. Alkaline Phosphatase (ALP) Activity

To confirm the effects of immobilized rhPDGF-BB, rhBMP-2, or rhPDGF-BB/rhBMP-2 on osteogenic differentiation, we evaluated the ALP activities and calcium contents, as early and late differentiation of MG-63 osteoblast-like cells, were evaluated, respectively. ALP activities were measured after culture for 3, 7, or 10 days. In brief, cells ( $1 \times 10^5$  cells/mL) were seeded on the surfaces of each Ti disc ( $n = 5$ ). At predesignated times, cells and Ti sample were washed with PBS.

Then, RIPA buffer (1×) containing protease and phosphatase inhibitor was added to cells. Cells were then lysed with RIPA (1×) buffer and centrifuged at 13,500 rpm for 1 min to remove cell debris. P-nitrophenyl phosphate solution was then added to supernatants and incubated for 30 min at 37 °C and 1 N NaOH was added to stop reactions. Optical densities of ALP were determined using a Flash Multimode Reader at 405 nm.

#### 2.4.2. Calcium Contents

To determine the calcium contents of MG-63 cells, cells were seeded at a density of  $1 \times 10^5$  cells/mL on the surfaces of each Ti disc ( $n = 5$ ) and cultured for 7 or 21 days. Ti discs were then rinsed with PBS, and treated with 0.5 N HCl for 24 h, the Ti discs containing cells were performed by centrifugation at 13,500 rpm for 1 min. Calcium contents were assessed by a QuantiChrom Calcium Assay Kit (DICA-500, BioAssay Systems, Hayward, CA, USA) using calcium chloride as a standard and a Flash Multimode Reader at 612 nm.

#### 2.4.3. Gene Expressions

To assess the osteogenic differentiation effects of different substrates, gene expressions of osteogenic differentiation markers, that is, osteocalcin (OCN) and osteopontin (OPN), were investigated by real-time PCR. Cells were seeded at  $1 \times 10^5$  cells/mL on Ti, PDGF/Hepa/Ti, BMP/Hepa/Ti, and PDGF/BMP/Hepa/Ti, and cultured for 7 or 21 days ( $n = 5$ ). RNA was extracted using the RNeasy Plus Mini Kit (Qiagen, Valencia, CA, USA). 1 µg of total RNA was reverse transcribed into cDNA using AccuPower RT PreMix (Bioneer, Daejeon, Korea), according to the manufacturer's protocol. Primer sequences of target genes were as follows: OCN (F) 5'-TTG GTG CAC ACC TAG CAG AC-3', (R) 5'-ACC TTA TTG CCC TCC TGC TT-3'; and OPN (F) 5'-GAG GGC TTG GTT GTC AGC-3', (R) 5'-CAA TTC TCA TGG TAG TGA GTT TTC C-3'. PCR amplification and detection were performed using an ABI7300 Real-Time Thermal Cycler (Applied Biosystems, Foster, CA, USA).

### 2.5. In Vivo Animal Study

#### 2.5.1. Fabrication of Implants

Forty implants (Ø 4.0 × H 8.0; Cowellmedi Co., Busan, Korea) were prepared for animal study. All of the the treated implants were fabricated by pure titanium (grade 4), and had microthreads on one end and broader threads on the other. Implant surfaces were anodized (Cowellmedi Co., Busan, Korea), and anodized implants were used as controls (Ti group), the experimental groups were as follows; the heparinized implant group (the Hepa/Ti group), the rhPDGF-BB (0.75 mg/mL) [33] immobilized implant group (the PDGF/Hepa/Ti group), the rhBMP-2 (0.75 mg/mL) immobilized implant group (BMP/Hepa/Ti group), and the rhPDGF-BB (0.75 mg/mL) plus rhBMP-2 (0.75 mg/mL) [34,35] immobilized implant group (PDGF/BMP/Hepa/Ti group). Eight implants were allocated to each group (a total of 40). To apply rhBMP-2/rhPDGF-BB coating, each implant was placed h in the protein solution for 12 (0.75 mg/mL for rhBMP-2, 0.75 mg/mL for rhPDGF-BB) up to its microthreads, and then freeze dried under sterile conditions (freeze dried at −40 °C, and then vacuum dried at ≤20 °C).

This study was carried out with the approval from the Ethics Committee on Animal Experimentation of Chun Nam University (CNU IACUC-TB-2010-10). Five three-year-old beagle dogs of weight 13–15 kg were used for this study. Animals were given two-weeks to acclimatize, fed a soft-dog food diet, and had free access to water.

#### 2.5.2. Surgical Procedures

At first surgery, premolars and first molars of upper and lower jaws were extracted. Animals were pre-anaesthetized with atropine sulfate induction (0.05 mg/kg IM; Dai Han Pharm Co., Seoul, Korea) and maintained on isoflurane (Choongwae Co., Seoul, Korea) gas anesthesia. Lidocaine (1 mL; Yu-Han Co., Gunpo, Korea) containing 1:100,000 epinephrine was infiltrated into mucosae at surgical

sites. The upper, lower premolars, and first molars were separated into mesial and distal roots. Care was taken to preserve the lateral, lingual, and buccal walls of alveolar sockets. Teeth were extracted carefully, and extraction sites were sutured with nylon silk (4-0, Mersilk, Ethicon Co., Livingston, UK) to enhance healing. The extraction sites were allowed to heal for two months.

Implant surgery was performed when extraction sockets had completely healed. The anesthetics (local and general) were performed, as described for first surgery. The implants of each groups were implanted at edentulous mandibular alveolar ridge. Briefly, each alveolar ridge was trimmed by ~1.5 mm to create a flat ridge before implant insertion, the buccal open defect model that had 2.5 mm depth was formed. This model was not buccal bone, and there was mesial-lingual-distal 1 mm defect area around 2.5 mm upper portion of implant (Figure 1a). Implants (control (Ti) group, Hepa/Ti group, PDGF/Hepa/Ti group, BMP/Hepa/Ti group, and PDGF/BMP/Hepa/Ti group) were installed randomly on right and left mandibular alveolar ridges (8 implants per dog). To place implants at the same position on both sides, exposed bone was marked at implant placement sites using a ruler. 5 mm of implant was placed within the reduced alveolar ridge to the reference notch level (shown on the implant), which resulted in a 2.5 mm peri-implant buccal open defects (Figure 1b,c). Each implant was covered with cover-screw. Mucoperiosteal flaps were advanced, adapted, and sutured leaving the implants submerged.

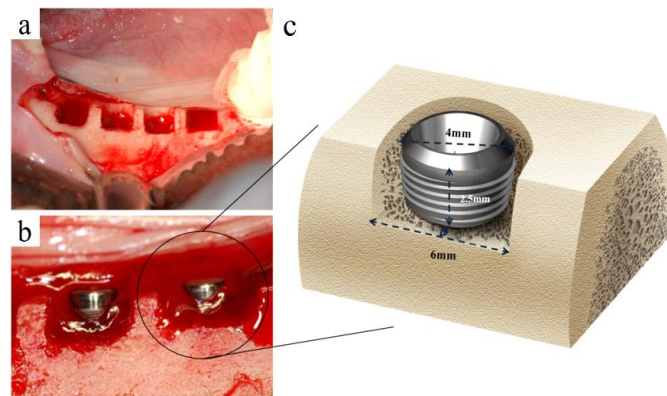


**Figure 1.** (a) Alveolar bone was flattened without exposing cancellous bone; (b) 5 mm of implant was placed within the reduced alveolar ridge and upper 2.5 mm of implants was placed in supra alveolar peri-implant buccal open defects; and (c) Schematic diagram of the buccal open defect model.

### 2.5.3. Post-Operative Care after Implant Placement and Sacrifice

A broad spectrum antibiotic (penicillin G with was administered immediately after implant placement and again 48 h later by intramuscular injection (1 mL/5 kg). To control the plaque, Teeth were washed out with 2% chlorhexidine gluconate every day until study completion. Observations of experimental sites with regards to mucosal health, edema, maintenance of suture closure, and tissue infection or necrosis were made daily until suture removal. Suture materials were removed one week after implant placement. Experimental animals were given a soft diet for two weeks, followed by a conventional regular diet. The animals were anesthetized and euthanized at eight weeks after implant placement by intravenous injection of concentrated sodium pentobarbital (Euthasol, Delmarva Laboratories Inc., Midlothian, VA, USA). Following euthanasia, block sections including implants, alveolar bone, and surrounding mucosa were collected.

### 2.5.4. Measurement of Implant Stability

Implant stability quotient (ISQ) values were measured to evaluate stability at the time of placement. ISQ values of all the implants placed in mandibles were measured immediately and at week eight after second surgery using Osstell Mentor® (Integritation Diagnostic Ltd., Göteborg, Sweden). ISQ values



were measured five times for each implant, and mean and standard deviations (SDs) were calculated after excluding minimum and maximum values.

### 2.5.5. Micro Computed Tomography ( $\mu$ CT)

The collected samples were fixed in phosphate-buffered formaldehyde (pH 7.4, 0.1 M PBS) and dehydrated in ethanol 70%. Three dimensional (3D)  $\mu$ CT images were obtained to determine bone mineral densities and bone volumes surrounding implants in defect areas. Specimens were wrapped using Parafilm M<sup>®</sup> (Pechiney Plastic Packaging, Chicago, IL, USA) to prevent dry during scanning, and scanned at 130 kV and 60  $\mu$ A with a resolution of 12  $\mu$ m pixels using a bromine filter (0.25 mm) (Skyscan-1173 Skyscan<sup>®</sup>, Kontich, Belgium). In addition, calibration rods of standard bone mineral densities were also scanned. Cone-beam reconstruction (version 2.15, Skyscan<sup>®</sup>, Kontich, Belgium) was performed, and all scan and reconstruction parameters that were applied were identical for all the specimens and calibration rods. The collected data were analyzed by a CT analyser (version 1.4, Skyscan<sup>®</sup>, Kontich, Belgium). The region of interest (ROI) was defined as annular region of thickness 1 mm surrounding a defect area in the marginal peri-implant from the first microthread to the last microthread. Bone volumes ( $\text{mm}^3$ ) were measured in this region (Figure 2) and were expressed as percentages of the total ROI volumes ( $\text{mm}^3$ ).

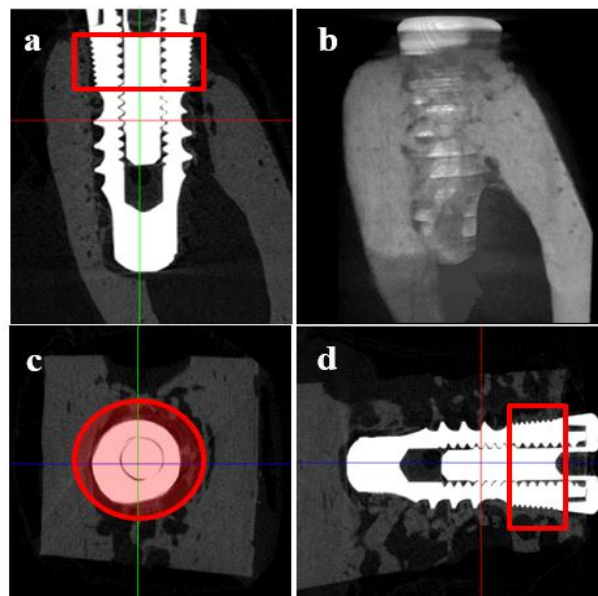


**Figure 2.** Micro-computed tomography ( $\mu$ CT) images in each group. (a) Buccolingual section image; (b) three-dimensional (3D) image; (c) Horizontal section image; and (d) Mesiodistal section image. Region of interest (ROI) was defined as an annular area of thickness 1 mm surrounding the defect area (red circle) in the marginal portion of the peri-implant from the first microthread to the last microthread. Bone volumes were measured in this ROI.

### 2.5.6. Histologic and Histometric Analysis

The harvested specimens were immersed in neutral buffered formalin (Sigma Aldrich, St Louis, MO, USA), fixed for two weeks, and dehydrated in ascending concentrations of ethanol (70%, 80%, 90%, and 100%), and embedded in Technovit 7200 VLC resin (Heraeus KULZER, South Bend, IN, USA). Embedded specimen blocks were sectioned longitudinally from the center of implant using a diamond cutter (KULZER EXAKT 300, EXAKT, Norderstedt, Germany). The final slides (30  $\mu$ m) were prepared from initial 400  $\mu$ m slides by grinding sections using a grinding machine (KULZER EXAKT 400CS, EXAKT, Norderstedt, Germany). Hematoxylin-eosin staining was performed, and images were captured by computer connected to light microscope (Olympus BX, Olympus, Tokyo, Japan) attached

to a CCD camera (Polaroid DMC2 digital Microscope camera (Polaroid Corporation, Cambridge, MA, USA). All assessments were made by one skilled investigator using SPOT Software (Ver. 4.0, Diagnostic Instrument, Inc., Sterling Heights, MI, USA).

The following parameters [36] were evaluated:

- Bone growth height in buccal defect areas (BG, mm): The thickness of bone that grew upward from the implant from the reference point on the buccal defect site on the alveolar ridge.
- Bone to implant contact in microthreads (microBIC, %): The bone to implant contact ratio was measured in buccal and lingual defect areas where the bone grew along the implant from the implantation reference point on the alveolar ridge.
- Bone to implant contact in macrothreads (macroBIC, %): The bone to implant contact ratio was measured in existing bone where the implant was implanted.
- Intra-thread bone density in macrothreads (ITBD, %): Intra-thread bone density was measured in the existing bone where the implant was placed.

After measuring the percentage of bone to implant contact (BIC, %), the ratio of bone formation area on intra-threads of implant to overall threads was calculated to determine intra-thread bone density (ITBD, %). Height of newly formed marginal bone by implants was measured. Images of specimens were captured at a magnification of  $\times 12.5$  and  $\times 40$ . For the histometric analysis, a magnification of  $\times 40$  was used.

#### 2.5.7. Statistical Analysis

All of the analyses were performed using statistical program (SPSS ver. 21.0). Mean and SDs of ISQ values and of BIC and ITBD values were calculated for each group. Comparisons of ISQ values between the experimental and control groups were made using the Mann-Whitney U test. The Shapiro-Wilk test was used to test the normalities of distributions, and then one-way ANOVA was used to compare group BICs, ITBDs, and bone growths. *Post hoc* testing was performed using Bonferroni's test using a significance level of 95%.

### 3. Results

#### 3.1. Characterization of Ti and Modified Ti Morphologies

##### 3.1.1. Scanning Electron Microscopy (SEM)

As shown in Figure 3, the surface morphologies of Ti, Hepa/Ti, PDGF/Hepa/Ti, BMP/Hepa/Ti, and PDGF/BMP/Hepa/Ti discs were investigated using SEM. Ti modified with rhHepa-DOPA, rhPDGF-BB, rhBMP-2, or rhPDGF-BB/rhBMP-2 had surface morphologies similar to Ti alone. These results indicate that the surfaces of Ti modified by small molecules, such as, Hepa-DOPA, rhPDGF-BB, rhBMP-2, or rhPDGF-BB/rhBMP-2 cannot be differentiated by SEM.

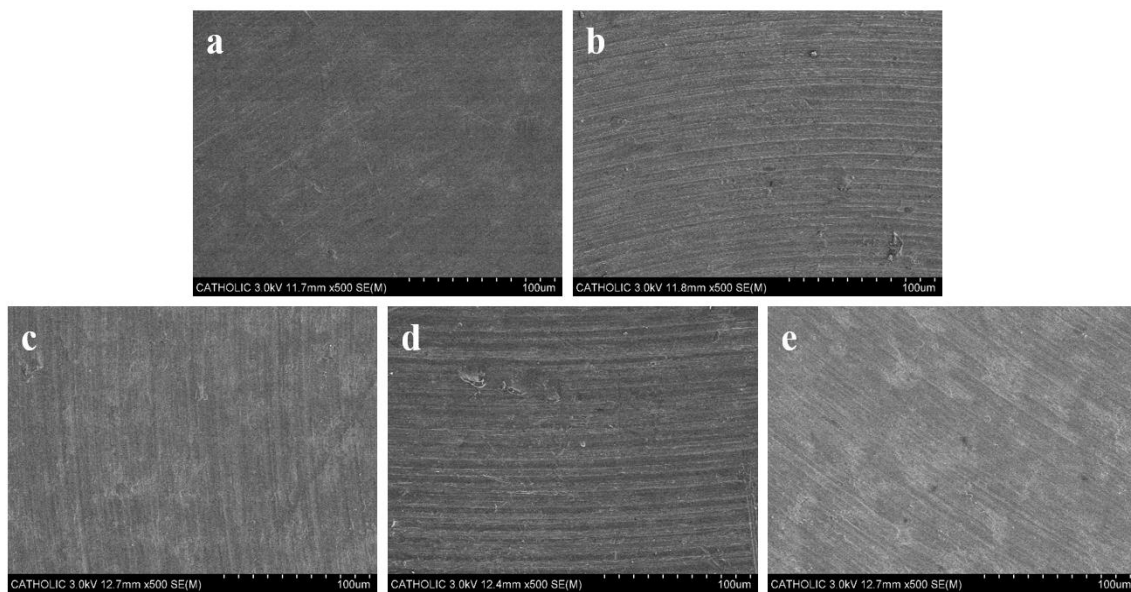


**Figure 3.** Scanning electron microscope (SEM) images of (a) Ti, (b) Hepa/Ti, (c) PDGF/Hepa/Ti, (d) BMP/Hepa/Ti, and (e) PDGF/BMP/Hepa/Ti.

### 3.1.2. X-ray Photoelectron Spectroscopy (XPS)

The surface chemical compositions of all Ti substrates determined by XPS are shown in Table 1. After anchoring Hepa-DOPA on the surface of Ti, C1s, and N1s peaks increased to compare with Ti alone. After immobilizing rhPDGF-BB and/or rhBMP-2 on the surface of Hepa/Ti disc, the N1s peak was increased and the S2p peak decreased versus Hepa/Ti. The amount of heparin anchored onto the Ti surface was  $1.62 \pm 0.32 \mu\text{g}/\text{disc}$ .

**Table 1.** Surface chemical compositions evaluated in 1 disc per group.

Specimen	C1s (%)	N1s (%)	O1s (%)	S2p (%)	Ti2p (%)	Total (%)
Ti	56.47	0.88	30.46	-	12.19	100
Hepa/Ti	62.01	3.01	28.63	0.56	5.79	100
PDGF/Hepa/Ti	60.86	5.28	30.23	0.36	3.27	100
BMP/Hepa/Ti	61.52	5.90	28.99	0.41	3.18	100
PDGF/BMP/Hepa/Ti	60.25	5.87	30.56	0.30	3.02	100

### 3.2. In Vitro rhPDGF-BB and rhBMP-2 Releases

The release behaviors of rhPDGF-BB or rhBMP-2 from PDGF/Hepa/Ti, BMP/Hepa/Ti, and PDGF/BMP/Hepa/Ti are shown in Figure 4, respectively. The amounts of rhPDGF-BB released from PDGF/Hepa/Ti and PDGF/BMP/Hepa/Ti discs were  $25.20 \pm 6.48 \text{ ng}$  and  $15.56 \pm 4.55 \text{ ng}$  after 1 day, respectively. Over 28 days, the amounts of rhPDGF-BB released were  $66.69 \pm 5.81 \text{ ng}$  for PDGF/Hepa/Ti and  $34.52 \pm 4.55 \text{ ng}$  for PDGF/BMP/Hepa/Ti. In addition, on day 1, the amounts of rhBMP-2 that is released from BMP/Hepa/Ti and PDGF/BMP/Hepa/Ti were  $27.46 \pm 6.71 \text{ ng}$  and  $16.56 \pm 4.48 \text{ ng}$ , respectively. Over the 28-day period, the amount of rhBMP-2 released was  $69.85 \pm 7.43 \text{ ng}$  for BMP/Hepa/Ti and  $37.52 \pm 4.26 \text{ ng}$  for PDGF/BMP/Hepa/Ti.



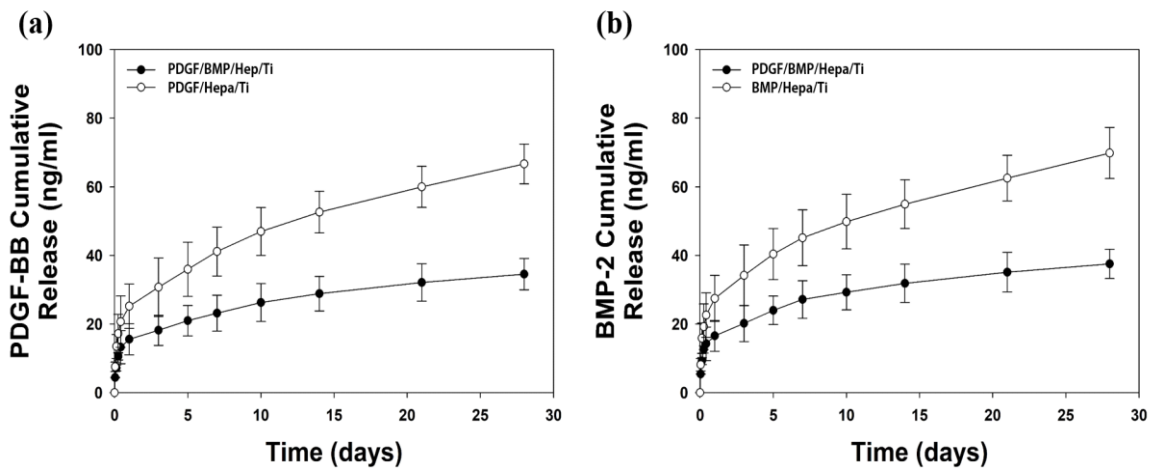


**Figure 4.** In vitro releases of (a) rhPDGF-BB and (b) rhBMP-2 from PDGF/Hepa/Ti, BMP/Hepa/Ti and PDGF/BMP/Hepa/Ti.

### 3.3. In Vitro Cell Study

#### 3.3.1. ALP Activity

ALP activities of MG-63 cells seeded on the surface of Ti, PDGF/Hepa/Ti, BMP/Hepa/Ti, and PDGF/BMP/Hepa/Ti discs were confirmed after 3, 7, and 10 days of culture (Figure 5a). On day 3, the ALP activities of cells cultured on PDGF/Hepa/Ti, BMP/Hepa/Ti, and PDGF/BMP/Hepa/Ti were higher than that of cells cultured on Ti. On days 7 and 10, the ALP activities of cells that are grown on PDGF/Hepa/Ti, BMP/Hepa/Ti, and PDGF/BMP/Hepa/Ti differed significantly from those grown on Ti alone. On days 7 and 10, the ALP activity of cells cultivated on BMP/Hepa/Ti was significantly higher than that of those cultivated on PDGF/Hepa/Ti or PDGF/BMP/Hepa/Ti.

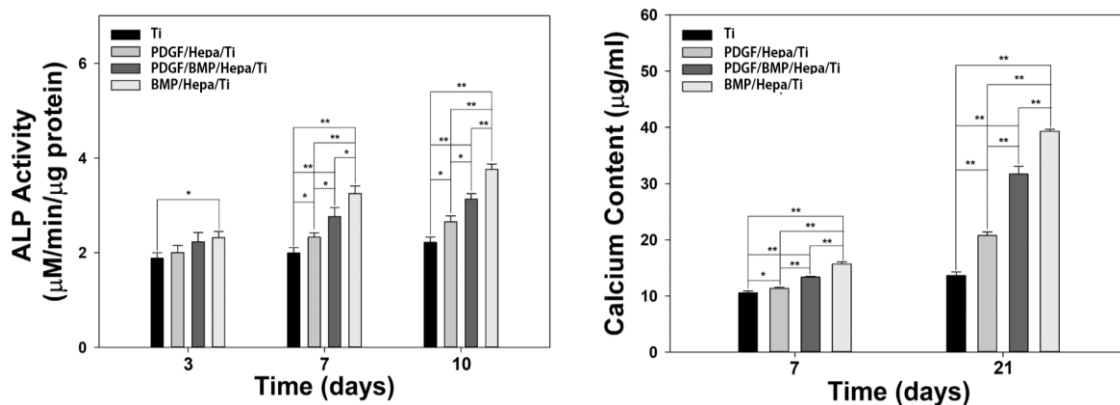


**Figure 5.** (a) Alkaline phosphatase (ALP) activities of cells cultured on Ti, PDGF/Hepa/Ti, BMP/Hepa/Ti, and PDGF/BMP/Hepa/Ti for 3, 7, or 10 days (\*  $p < 0.05$  and \*\*  $p < 0.01$ ); (b) Calcium contents of cells grown on Ti, PDGF/Hepa/Ti, BMP/Hepa/Ti, and PDGF/BMP/Hepa/Ti for 7 or 21 days (\*  $p < 0.05$  and \*\*  $p < 0.01$ ).

#### 3.3.2. Calcium Contents

The calcium contents of MG-63 cells cultured on Ti, PDGF/Hepa/Ti, BMP/Hepa/Ti, and PDGF/BMP/Hepa/Ti discs for 7 and 21 days are shown in Figure 4. The calcium contents of cells cultivated on PDGF/Hepa/Ti, BMP/Hepa/Ti, and PDGF/BMP/Hepa/Ti were significantly greater than those that were grown on Ti alone on days 7 and 21. Moreover, the calcium contents of

cells grown on BMP/Hepa/Ti and PDGF/Hepa/Ti and on BMP/Hepa/Ti and PDGF/BMP/Hepa/Ti differed significantly.

### 3.3.3. Gene Expressions

After 7 and 21 days of culture, the mRNA expression levels of OCN and OPN in cells grown on Ti disc or on Ti modified with rhPDGF-BB and/or rhBMP-2 were determined by real-time PCR (Figure 6). mRNA expression levels of OCN and OPN in cells cultured on BMP/Hepa/Ti or PDGF/BMP/Hepa/Ti were markedly higher than in those cultured on Ti alone at day 7. In addition, OCN and OPN expressions in cells cultivated on PDGF/Hepa/Ti were greater than in those cultivated on Ti alone at day 7, but not significantly so. On day 21, the expression levels of OCN and OPN in cells that are grown on Hepa/Ti immobilized with rhPDGF-BB and/or rhBMP-2 and Ti alone were significantly different, as were OCN and OPN expressions in cells cultivated on BMP/Hepa/Ti and PDGF/Hepa/Ti or PDGF/BMP/Hepa/Ti discs.

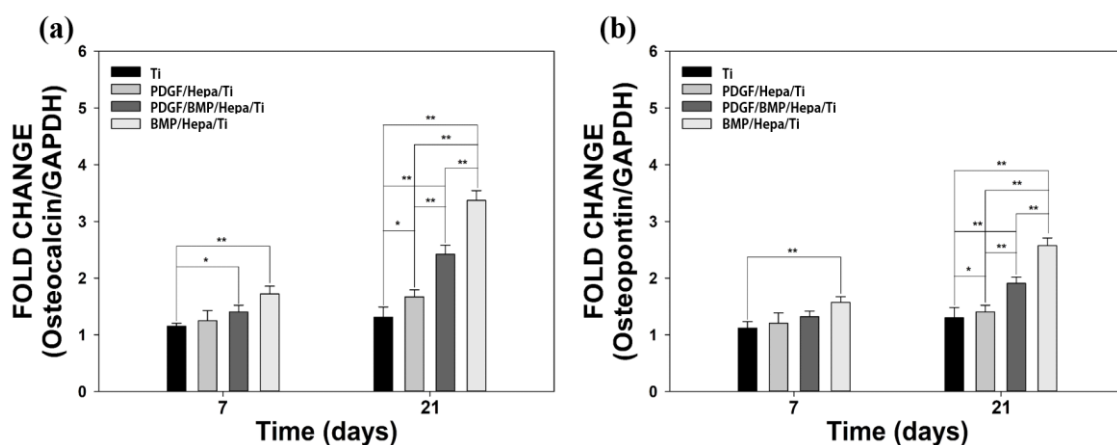


**Figure 6.** Real-time PCR analysis of the mRNA levels of (a) osteocalcin and (b) osteopontin in cells grown on Ti, PDGF/Hepa/Ti, BMP/Hepa/Ti, or PDGF/BMP/Hepa/Ti discs for 7 or 21 days (\*  $p < 0.05$  and \*\*  $p < 0.01$ ).

## 3.4. In Vivo Animal Study

### 3.4.1. Clinical Findings

All of the experimental animals survived during the healing procedure, and there was no observation of infection or inflammation at surgical sites. Samples of 40 implants were collected without any issue for in vivo  $\mu$ CT and Histomorphometric analysis.

### 3.4.2. Stability Evaluation

Immediately after implantation, the ISQ values in all of the experimental groups were higher than in control group, but differences were not statistically significant. At eight weeks after surgery, ISQ values were higher than at baseline in the experimental groups, whereas in the control group, they were lower or similar than baseline values. ISQ increases were significantly greater in the experimental groups than in the control group ( $p < 0.05$ ) (Table 2). But, no difference was observed between the groups ( $p > 0.05$ ).

**Table 2.** Implant stability quotient (ISQ) values of groups immediately and 8 weeks after implantation.

Group	At Surgery	At 8 Weeks	ISQ Change
Ti	70.00 ± 4.45 <sup>a</sup>	71.27 ± 7.67 <sup>a</sup>	0.27 ± 7.97 <sup>a</sup>
Hepa/Ti	70.59 ± 8.17 <sup>a</sup>	70.70 ± 5.78 <sup>a</sup>	0.01 ± 9.19 <sup>a</sup>
PDGF/Hepa/Ti	69.99 ± 5.12 <sup>a</sup>	71.01 ± 4.98 <sup>a</sup>	0.92 ± 8.32 <sup>a</sup>
BMP/Hepa/Ti	71.33 ± 6.82 <sup>a</sup>	77.14 ± 5.23 <sup>b</sup>	5.32 ± 5.33 <sup>b</sup>
PDGF/BMP/Hepa/Ti	70.43 ± 6.44 <sup>a</sup>	81.41 ± 5.11 <sup>b</sup>	8.11 ± 7.09 <sup>b</sup>
* <i>p</i>	0.1255	0.0201	0.0011

Notes: At surgery: ISQ value at surgery; At week 8: ISQ value 8 weeks after surgery; <sup>a,b</sup>: Numbers in the same column with the same superscripts were not significantly different; *p* values were obtained by ANOVA; \**p* < 0.05.

### 3.4.3. Micro Computed Tomography (μCT)

Mean bone volume (%) in the control group was 18.19 ± 4.39% and in the Hepa/Ti, PDGF/Hepa/Ti, BMP/Hepa/Ti, and PDGF/BMP/Hepa/Ti groups mean bone volumes were 13.05 ± 5.15, 21.29 ± 9.56, 40.95 ± 9.07, and 43.73 ± 6.75%, respectively (Figure 7; *n* = 8). Bone volumes in the BMP/Hepa/Ti and PDGF/BMP/Hepa/Ti groups were significantly higher than in the other groups (*p* < 0.05). But, there was no significant difference between the BMP/Hepa/Ti and PDGF/BMP/Hepa/Ti groups (*p* > 0.05).

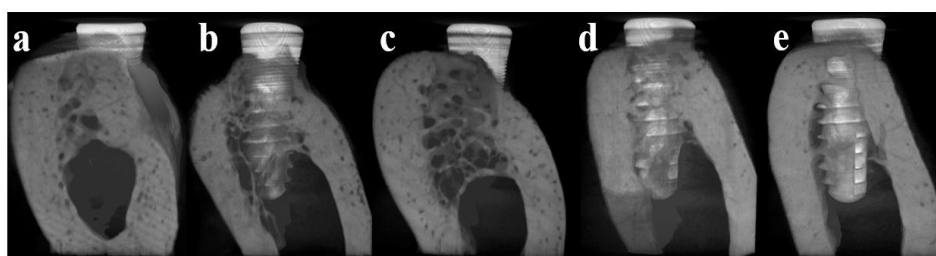


**Figure 7.** μCT 3D images of the five study groups. (a) Ti group; (b) Hepa/Ti group; (c) PDGF/Hepa/Ti group; (d) BMP/Hepa/Ti group; and (e) PDGF/BMP/Hepa/Ti group (×12.5 magnification). Note pronounced re-modeling of peri-implant bone and vertical bone growth in the BMP/Hepa/Ti and PDGF/Hepa/Ti groups. No bone growth was observed in defect areas in the Ti, Hepa/Ti, and PDGF/Hepa/Ti groups.

### 3.4.4. Histomorphometric Analysis

Jaw quadrants in the BMP/Hepa/Ti and PDGF/BMP/Hepa/Ti groups exhibited bone formation approaching microthreads and bone remodeling around implants (Figure 8). There was about 1.1 mm more bone gain in the BMP/Hepa/Ti and PDGF/BMP/Hepa/Ti groups than in the control group (*p* < 0.05). In the control and heparin groups, vertical bone loss was observed in buccal defect areas. The control, heparin, and PDGF groups showed failure of osseointegration in lingual regions observed a 1 mm gap between fixture and bone (Figure 9). The microBIC values of the BMP/Hepa/Ti and PDGF/BMP/Hepa/Ti groups were significantly greater than those of the other groups (*p* < 0.05), but no significant difference was observed between the BMP/Hepa/Ti and PDGF/BMP/Hepa/Ti groups (*p* > 0.05). The BMP/Hepa/Ti and PDGF/BMP/Hepa/Ti groups showed successful osseointegration in lingual portions (Figure 10). Mean group percentages (±SD) of BIC and ITBD within macrothreads eight weeks after surgery were not significantly different (*p* > 0.05) (Table 3).

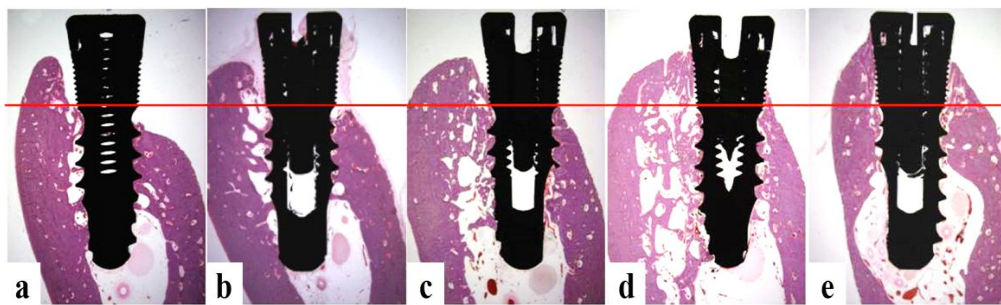


**Figure 8.** Histological specimens of the five groups. (a) Ti group; (b) Hepa/Ti group; (c) PDGF/Hepa/Ti group; (d) BMP/Hepa/Ti group; and (e) PDGF/BMP/Hepa/Ti group ( $\times 12.5$  magnification). Note pronounced peri-implant bone re-modeling and vertical bone growth in the BMP/Hepa/Ti and PDGF/BMP/Hepa/Ti groups. Red lines indicate defect levels.

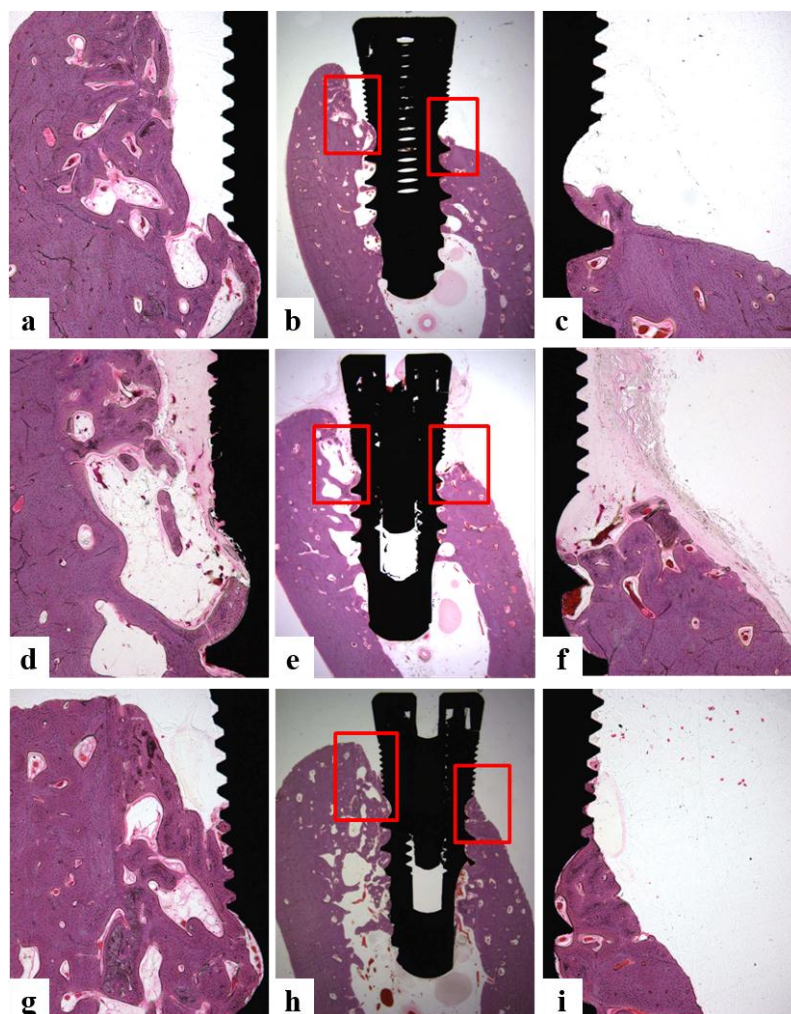


**Figure 9.** Microthread defect areas in the control (Ti), Hepa/Ti and PDGF/Hepa/Ti groups. Group BIC and ITBD within macrothreads at 8 weeks after surgery were not significantly different. In the control and heparin groups, vertical bone loss was detected in buccal defect areas. Failure of osseointegration in the lingual portion observed as a 1 mm gap between fixture and bone was present in the control, heparin, and PDGF groups. (a–c) Ti group; (d–f) Hepa/Ti group; (g–i) PDGF/Hepa/Ti group; (a,d,g) lingual portion of microthread; and (c,f,i) buccal portion of microthread. (a,c,d,f,g,i)  $\times 40$  magnification, (b,e,h)  $\times 12.5$  magnification.



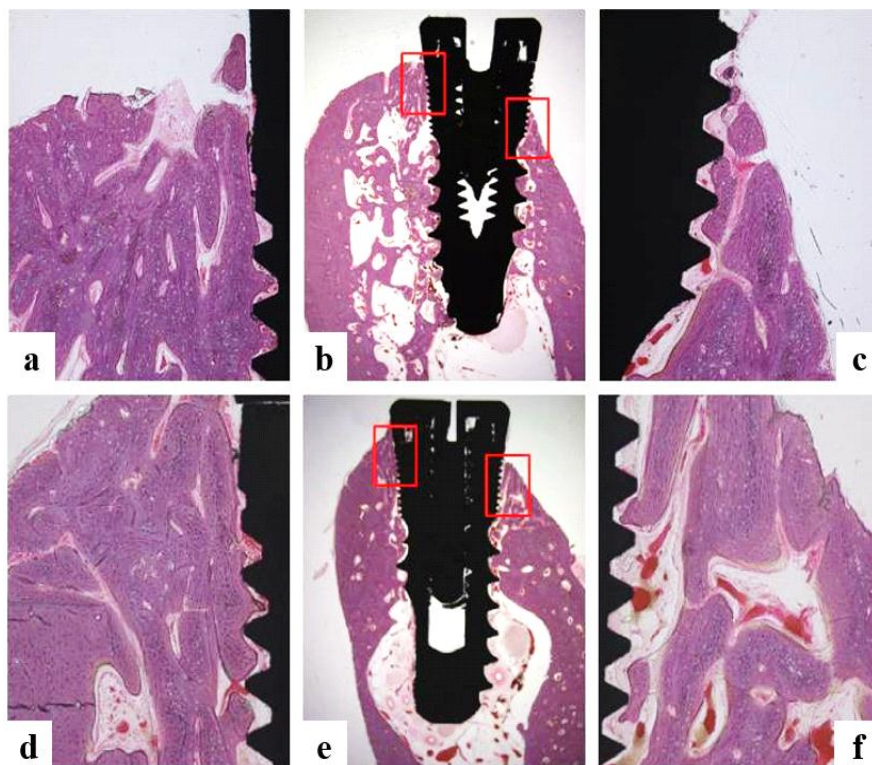


**Figure 10.** Microthread defect area in the BMP/Hepa/Ti and PDGF/BMP/Hepa/Ti groups. The BMP/Hepa/Ti and PDGF/BMP/Hepa/Ti group exhibited successful osseointegration in lingual portions. (a,d) lingual microthread portion; (c,f) buccal microthread portion; (a–c) BMP/Hepa/Ti group; (d–f) PDGF/BMP/Hepa/Ti group. (a,c,d,f)  $\times 40$  magnification, (b,e)  $\times 12.5$  magnification.

**Table 3.** Results of histometric analysis performed at 8 weeks after surgery. (Buccal bone level, BIC on macrothreads, and bone density on macrothreads;  $n = 8$ ).

Group	BG (mm)	microBIC (%)	macroBIC (%)	ITBD (%)
Ti	$0.23 \pm 0.22^a$	$11.05 \pm 5.09^a$	$23.58 \pm 1.63^a$	$54.90 \pm 7.24^a$
Hepa/Ti	$-0.06 \pm 0.21^a$	$9.27 \pm 1.95^a$	$18.47 \pm 2.89^a$	$53.98 \pm 3.77^a$
PDGF/Hepa/Ti	$0.12 \pm 0.28^a$	$9.59 \pm 3.99^a$	$20.62 \pm 2.30^a$	$61.64 \pm 6.17^a$
BMP/Hepa/Ti	$1.34 \pm 0.17^b$	$27.76 \pm 3.03^b$	$22.20 \pm 2.89^a$	$60.80 \pm 3.32^a$
PDGF/BMP/Hepa/Ti	$1.31 \pm 0.12^b$	$31.79 \pm 3.90^b$	$23.54 \pm 2.30^a$	$69.22 \pm 3.96^a$
* <i>p</i>	0.000	0.000	0.544	0.244

Notes: BG: Bone growth height in buccal defect area (mm); microBIC: Bone to implant contact in the microthreads (%); macroBIC: Bone to implant contact in macrothreads (existing bone area around implant, %); ITBD: Intra-thread bone density in macrothreads (existing bone area around implant, %); <sup>a,b</sup>: Means with the same superscripts in same columns were not significantly different; *p* values were obtained by ANOVA; \**p* < 0.05.

#### 4. Discussion

Many studies have been conducted on implant surfaces treated with growth factors like BMP-2, to increase vertical and horizontal bone regeneration without the use of additional bone grafts or barrier membranes [37,38]. Although BMP-2 is one of the effective growth factors, rapid release at an early stage and rapid diffusion into body fluids has limited its clinical applications [39,40]. In order to overcome these problems, the present study was undertaken on a heparin-based release system to provide the sustained and local release of BMP-2 [30,41,42]. Since titanium has good mechanical properties, corrosion resistance, and biocompatibility without biological activity, it is generally used as an implant material [43]. Due to its inertness in vivo, physical adsorption or chemical coatings are



required to enable biomolecules to adhere to titanium surfaces [44]. However, the chemical substances used for this purpose, such as, APTES, EDAC, and NHS, are harmful to the human body [45]. In this study, titanium was coated with heparin using a dopamine surface modification technique, which has been reported to be biocompatible in *in vivo* toxicity studies [46]. Dopamine is a small molecule substance that possesses catechol and amine functional groups [47]. The catechol component bonds to titanium oxide surfaces and provides an amine group that can bind heparin [48,49].

It has been reported that combinations of different growth factors produce synergistic effects that promote the complex cellular activities that occur during bone regeneration and osseointegration [33,50,51]. However, most studies are limited to cell experiments, the studies reproducing the clinical situation in large animals are rare. Therefore, in the present study, rhBMP-2 and rhPDGF-BB immobilized on Ti surfaces modified with Hepa-DOPA were utilized to establish an effective growth factor delivery system to ensure sustained factor release in appropriate amounts over sufficient time in beagle mandible model. The concentration of rhBMP-2 that is used in this study was set based on our previous studies, which reported 0.75 mg/mL of rhBMP-2 is effective on bone regeneration [34,35]. In PDGF, the previous study of Choo et al. [33] reported that the appropriate concentration of PDGF was from 0.3 mg/mL up to 1 mg/mL, thus we chose 0.75 mg/mL of PDGF concentration within that range. BMP and PDGF combined groups were studied in 1:10 ratio (PDGF:BMP) in previous cell study [6], but we intended to increase the rate of PDGF to get enhanced bone regeneration as ratio of 1:1. The results of our *in vitro* release experiments indicated that the inclusion of heparin achieved sustained growth factor release, although previous studies have reported a burst release pattern resulting in the release of 70%–90% over the first 6 h [52]. After 24 h, the amounts of PDGF-BB and rhBMP released from PDGF/Hepa/Ti and BMP/Hepa/Ti were approximately 38%, respectively, and the amounts of rhBMP and PDGF-BB released from PDGF/BMP/Hepa/Ti were 45%, respectively. This suggests that PDGF-BB and rhBMP-2 show similar release tendencies in the presence of other growth factors and heparin.

SEM analysis of Ti surface modified by heparin, rhPDGF-BB, or/and rhBMP-2 showed their surface morphologies were similar to that of untreated Ti. XPS showed heparin was successfully grafted on anodized Ti surfaces, as indicated by higher C and N peaks. In a previous study, successful immobilization of rhBMP-2 on surface of carboxymethyl chitosan (CMCS)-grafted Ti was attributed to the covalent bonds formation between the carboxyl groups of CMCS and the amine groups of rhBMP-2 [53]. In the present study, successful anchoring of rhBMP-2 and rhPDGF-BB to Hepa/Ti surfaces was demonstrated by further increases in N content.

ALP activity and calcium deposition as determined by *in vitro* studies are widely used as markers of early and late differentiation to osteoblasts, respectively [54,55]. We measured ALP activity after culturing MG-63 for 3, 7, or 10 days and calcium deposition after 7 or 21 days. ALP activities of cells that are cultured on PDGF-BB and/or BMP/Hepa/Ti were found to be significantly higher than those of cells cultured on untreated Ti on days 7 and 10 (\*  $p < 0.05$  and \*\*  $p < 0.01$ ). As reported in a previous study [6,56], our finding confirmed that rhBMP-2 and rhPDGF-BB both stimulate osteoblast differentiation. Furthermore, the calcium contents of cells cultured on PDGF-BB or/and BMP/Hepa/Ti were significantly higher than those of cells cultured on untreated Ti on days 7 and 21 (\*  $p < 0.05$  and \*\*  $p < 0.01$ ). These results indicate that growth factor immobilized Ti substrates can stimulate matrix formation and improve osteoblast cell function. ALP activity and calcium deposition in the PDGF/BMP/Hepa/Ti group were significantly higher than in the PDGF/Hepa/Ti group, but were significantly lower than in the BMP/Hepa/Ti group. In order to investigate the gene expression levels of osteocalcin (OCN) and osteopontin (OPN), which are markers of cell differentiation, the total mRNAs of cells cultured on four Ti surfaces were extracted. On day 21, significant differences were observed between the OCN and OPN expressions of cells cultivated on BMP/Hepa/Ti and PDGF/Hepa/Ti or PDGF/BMP/Hepa/Ti.

In the result of previous cell studies [6], PDGF-BB (5 ng/mL)/BMP-2(50 ng/mL)/Hepa/Ti (a 1:10 ratio of growth factors) was significantly higher than BMP/Hepa/Ti, whereas in this study, PDGF-BB

(50 ng/mL)/BMP-2 (50 ng/mL)/Hepa/Ti (a 1:1 ratio) was significantly lower than BMP/Hepa/Ti. Furthermore, ALP, calcium deposition, and gene expression not synergistically increased by the copresence of rhPDGF-BB and rhBMP-2. These results indicate that different concentrations and ratios of PDGF-BB should be selected.

The in vivo animal study was conducted to evaluate the synergic effects of rhBMP-2 (0.75 mg/mL) when combined with rhPDGF-BB (0.75 mg/mL). A total of 40 implants of five groups (control (Ti) group, Hepa/Ti group, PDGF/Hepa/Ti group, BMP/Hepa/Ti group, and PDGF/BMP/Hepa/Ti group) were implanted without using additional implants or barrier membranes. To reproduce clinical situations, a buccal open defect model with a 2.5 mm deep peri-implant bone defect was produced in the mandibles of five beagle dogs. This model was designed with loss of buccal bone and a mesial-lingual-distal 1 mm defect area around the 2.5 mm upper portions of implants. The upper part of implants (microthread) was exposed 2.5 mm above alveolar bone and the lower part (macrothread) was implanted into cortical bone. After a healing period of eight weeks, ISQ values showed the presences of rhBMP-2 and rhPDGF-BB contributed positively to implant stability. Furthermore, ISQ increases were significantly higher in the PDGF/BMP/Hepa/Ti and BMP/Hepa/Ti groups than in the other three groups (\*  $p < 0.05$ ). However, there was no difference between these two experimental groups ( $p > 0.05$ ).  $\mu$ CT analysis showed new bone volumes in the BMP/Hepa/Ti and PDGF/BMP/Hepa/Ti groups were significantly greater than in the other groups (\*  $p < 0.05$ ), but no significant difference was observed between these two groups ( $p > 0.05$ ). Our histomorphometric analysis confirmed vertical new bone formation and osseointegration approaching microthreads around peri-implant bone defects in the BMP/Hepa/Ti and PDGF/BMP/Hepa/Ti groups, whereas osseointegration was unsuccessful in the Ti, Hepa/Ti and PDGF/Hepa/Ti groups, in which a 1 mm gap between implant fixture and bone was observed at lingual portions. microBIC values in the BMP/Hepa/Ti and PDGF/BMP/Hepa/Ti groups were significantly greater than in the other groups (\*  $p = 0.000$ ), but no significant difference was observed between the two ( $p > 0.05$ ). Our in vivo studies were confirmed that PDGF (0.75 mg/mL)/BMP (0.75 mg/mL)/Hepa/Ti (a 1:1 growth factor) had no synergic effect. Based on these results and limitations of present study, further studies on subdivided concentrations and ratios, various implant surfaces and slow releasing systems are required to more comprehensively investigate the effects of combinations of different growth factors on osseointegration and bone regeneration.

## 5. Conclusions

Anodized Ti surfaces were successfully functionalized by surface grafting heparin and subsequently immobilizing rhBMP-2 and/or rhPDGF-BB. rhBMP-2 immobilized, heparin-grafted Ti implants were found to provide a suitable delivery system that enhanced osseointegration and bone regeneration in defect areas around implants. However, the study failed to reveal any synergetic effect resulting from the co-immobilization of rhBMP-2 and rhPDGF-BB.

**Acknowledgments:** This study was supported by a National Research Foundation of Korea (NRF) grant funded by the Korea government (MSIP) (No. 2017R1A2B4005820).

**Author Contributions:** Jung-Bo Huh conceived and designed the experiments; So-Hyoun Lee, Eun-Bin Bae, Sung-Eun Kim, Young-Pil Yun, Hak-Jun Kim, Jae-Won Choi and Jin-Ju Lee performed the experiments; So-Hyoun Lee, Sung-Eun Kim, Young-Pil Yun, Hak-Jun Kim and Jung-Bo Huh analyzed the data; So-Hyoun Lee, Eun-Bin Bae, and Jung-Bo Huh wrote the paper.

**Conflicts of Interest:** The authors have no conflict of interest to declare.

## References

1. Poli, P.P.; Beretta, M.; Cicciù, M.; Maiorana, C. Alveolar ridge augmentation with titanium mesh. A retrospective clinical study. *Open Dent. J.* **2014**, *8*, 148–158. [[PubMed](#)]
2. Retzepi, M.; Lewis, M.P.; Donos, N. Effect of diabetes and metabolic control on de novo bone formation following guided bone regeneration. *Clin. Oral Implants Res.* **2010**, *21*, 71–79. [[CrossRef](#)] [[PubMed](#)]

3. Rabel, A.; Köhler, S.G.; Schmidt-Westhausen, A.M. Clinical study on the primary stability of two dental implant systems with resonance frequency analysis. *Clin. Oral Investig.* **2007**, *11*, 257–265. [[CrossRef](#)] [[PubMed](#)]
4. Chen, D.; Zhao, M.; Mundy, G.R. Bone morphogenetic proteins. *Growth Factors* **2004**, *22*, 233–241. [[CrossRef](#)] [[PubMed](#)]
5. Hall, J.; Sorensen, R.G.; Wozney, J.M.; Wikesjo, U.M. Bone formation at rhBMP-2-coated titanium implants in the rat ectopic model. *J. Clin. Periodontol.* **2007**, *34*, 444–451. [[CrossRef](#)] [[PubMed](#)]
6. Kim, S.E.; Yun, Y.P.; Lee, J.Y.; Shim, J.S.; Park, K.; Huh, J.B. Co-delivery of platelet-derived growth factor (PDGF-BB) and bone morphogenetic protein (BMP-2) coated onto heparinized titanium for improving osteoblast function and osteointegration. *J. Tissue Eng. Regen. Med.* **2015**, *9*, E219–E228. [[CrossRef](#)] [[PubMed](#)]
7. Bessa, P.C.; Casal, M.; Reis, R.L. Bone morphogenetic proteins in tissue engineering: The road from laboratory to clinic, part II (BMP delivery). *J. Tissue Eng. Regen. Med.* **2008**, *2*, 81–96. [[CrossRef](#)] [[PubMed](#)]
8. Bessa, P.C.; Casal, M.; Reis, R.L. Bone morphogenetic proteins in tissue engineering: The road from the laboratory to the clinic, part I (basic concepts). *J. Tissue Eng. Regen. Med.* **2008**, *2*, 1–13. [[CrossRef](#)] [[PubMed](#)]
9. Becker, J.; Kirsch, A.; Schwarz, F.; Chatzinikolaidou, M.; Rothamel, D.; Lekovic, V.; Jennissen, H.P. Bone apposition to titanium implants biocoated with recombinant human bone morphogenetic protein-2 (rhBMP-2). A pilot study in dogs. *Clin. Oral Investig.* **2006**, *10*, 217–224. [[CrossRef](#)] [[PubMed](#)]
10. Wikesjo, U.M.E.; Xiropaidis, A.V.; Qahash, M.; Lim, W.H.; Sorensen, R.G.; Rohrer, M.D.; Wozney, M.; Hall, J. Bone formation at recombinant human bone morphogenetic protein-2-coated titanium implants in the posterior mandible (Type II bone) in dogs. *J. Clin. Periodontol.* **2008**, *35*, 985–991. [[CrossRef](#)] [[PubMed](#)]
11. Stenport, V.F.; Johansson, C.; Heo, S.J.; Aspenberg, P.; Albrektsson, T. Titanium implants and BMP-7 in bone: An experimental model in the rabbit. *J. Mater. Sci. Mater. Med.* **2003**, *14*, 247–254. [[CrossRef](#)] [[PubMed](#)]
12. Schliephake, H.; Aref, A.; Scharnweber, D.; Bierbaum, S.; Roessler, S.; Sewing, A. Effect of immobilized bone morphogenetic protein 2 coating of titanium implants on peri-implant bone formation. *Clin. Oral Implants Res.* **2005**, *16*, 563–569. [[CrossRef](#)] [[PubMed](#)]
13. Park, J.; Lutz, R.; Felszeghy, E.; Wiltfang, J.; Nkenke, E.; Neukam, F.W.; Schlegel, K.A. The effect on bone regeneration of a liposomal vector to deliver BMP-2 gene to bone grafts in peri-implant bone defects. *Biomaterials* **2007**, *28*, 2772–2782. [[CrossRef](#)] [[PubMed](#)]
14. Stadlinger, B.; Pilling, E.; Huhle, M.; Mai, R.; Bierbaum, S.; Scharnweber, D.; Kuhlisch, E.; Loukota, R.; Eckelt, U. Evaluation of osseointegration of dental implants coated with collagen, chondroitin sulphate and BMP-4: An animal study. *Int. J. Oral Maxillofac. Surg.* **2008**, *37*, 54–59. [[CrossRef](#)] [[PubMed](#)]
15. Ortolani, E.; Guerriero, M.; Coli, A.; Di Giannuario, A.; Minniti, G.; Polimeni, A. Effect of PDGF, IGF-1 and PRP on the implant osseointegration. A histological and immunohistochemical study in rabbits. *Ann. Stomatol. (Roma)* **2014**, *5*, 66–68. [[CrossRef](#)] [[PubMed](#)]
16. Chung, S.M.; Jung, I.K.; Yoon, B.H.; Choi, B.R.; Kim, D.M.; Jang, J.S. Evaluation of Different Combinations of Biphasic Calcium Phosphate and Growth Factors for Bone Formation in Calvarial Defects in a Rabbit Model. *Int. J. Periodontics Restor. Dent.* **2016**, *36*, s49–s59. [[CrossRef](#)] [[PubMed](#)]
17. Deshpande, A.; Koudale, S.B.; Bhongade, M.L. A comparative evaluation of rhPDGF-BB +  $\beta$ -TCP and subepithelial connective tissue graft for the treatment of multiple gingival recession defects in humans. *Int. J. Periodontics Restor. Dent.* **2014**, *34*, 241–249. [[CrossRef](#)] [[PubMed](#)]
18. Ridgway, H.K.; Mellonig, J.T.; Cochran, D.L. Human histologic and clinical evaluation of recombinant human platelet-derived growth factor and beta-tricalcium phosphate for the treatment of periodontal intraosseous defects. *Int. J. Periodontics Restor. Dent.* **2008**, *28*, 171–179.
19. Thakare, K.; Deo, V. Randomized controlled clinical study of rhPDGF-BB +  $\beta$ -TCP versus HA +  $\beta$ -TCP for the treatment of infrabony periodontal defects: Clinical and radiographic results. *Int. J. Periodontics Restor. Dent.* **2012**, *32*, 689–696.
20. Mishra, A.; Mishra, H.; Pathakota, K.R.; Mishra, J. Efficacy of modified minimally invasive surgical technique in the treatment of human intrabony defects with or without use of rhPDGF-BB gel: A randomized controlled trial. *J. Clin. Periodontol.* **2013**, *40*, 172–179. [[CrossRef](#)] [[PubMed](#)]
21. Deschaseaux, F.; Sensebe, L.; Heymann, D. Mechanisms of bone repair and regeneration. *Trends Mol. Med.* **2009**, *15*, 417–429. [[CrossRef](#)] [[PubMed](#)]

22. Misch, C.M.; Nevins, M.L.; Boch, J.A. Recombinant Human Bone Morphogenetic Protein-2 or Recombinant Human Platelet-Derived Growth Factor BB in Extraction Site Preservation and Bone Augmentation. In *Minimally Invasive Dental Implant Surgery*; Wiley-Blackwell: Hoboken, NJ, USA, 2015; pp. 119–136.
23. Pountos, I.; Georgouli, T.; Henshaw, K.; Bird, H.; Giannoudis, P.V. Release of growth factors and the effect of age, sex, and severity of injury after long bone fracture. *Acta Orthop.* **2013**, *84*, 65–70. [[CrossRef](#)] [[PubMed](#)]
24. Caplan, A.L.; Correa, D. PDGF in bone formation and regeneration: New insights into a novel mechanism involving MSCs. *J. Orthop. Res.* **2011**, *29*, 1795–1803. [[CrossRef](#)] [[PubMed](#)]
25. Centrella, M.; McCarthy, T.L.; Kusmik, W.F.; Canalis, E. Relative binding and biochemical effects of heterodimeric and homodimeric isoforms of platelet-derived growth factor in osteoblast-enriched cultures from fetal rat bone. *J. Cell. Physiol.* **1991**, *147*, 420–426. [[CrossRef](#)] [[PubMed](#)]
26. Hollinger, J.O.; Onikepe, A.O.; MacKrell, J.; Einhorn, T.; Bradica, G.; Lynch, S.; Hart, C.E. Accelerated fracture healing in the geriatric, osteoporotic rat with recombinant human platelet-derived growth factor-bb and an injectable beta-tricalcium phosphate/collagen matrix. *J. Orthop. Res.* **2008**, *26*, 83–90. [[CrossRef](#)] [[PubMed](#)]
27. Mitlak, B.H.; Finkelman, R.D.; Hill, E.L.; Li, J.; Martin, B.; Smith, T.; D’Andrea, M.; Antoniadis, H.N.; Lynch, S.E. The effect of systemically administered PDGF-BB on the rodent skeleton. *J. Bone Miner. Res.* **1996**, *11*, 238–247. [[CrossRef](#)] [[PubMed](#)]
28. Martino, M.M.; Briquez, P.S.; Ranga, A.; Lutolf, M.P.; Hubbell, J.A. Heparin-binding domain of fibrin (ogen) binds growth factors and promotes tissue repair when incorporated within a synthetic matrix. *Proc. Natl. Acad. Sci. USA* **2013**, *110*, 4563–4568. [[CrossRef](#)] [[PubMed](#)]
29. Perets, A.; Baruch, Y.; Weisbuch, F.; Shoshany, G.; Neufeld, G.; Cohen, S. Enhancing the vascularization of three-dimensional porous alginate scaffolds by incorporating controlled release basic fibroblast growth factor microspheres. *J. Biomed. Mater. Res. A* **2003**, *65*, 489–497. [[CrossRef](#)] [[PubMed](#)]
30. Ishibe, T.; Goto, T.; Kodama, T.; Miyazaki, T.; Kobayashi, S.; Takahashi, T. Bone formation on apatite-coated titanium with incorporated BMP-2/heparin in vivo. *Oral Surg. Oral Med. Oral Pathol. Oral Radiol. Endod.* **2009**, *108*, 867–8975. [[CrossRef](#)] [[PubMed](#)]
31. Lee, S.H.; Jo, J.Y.; Yun, M.J.; Jeon, Y.C.; Huh, J.B.; Jeong, C.M. Effect of immobilization of the recombinant human bone morphogenetic protein 2 (rhBMP-2) on anodized implants coated with heparin for improving alveolar ridge augmentation in beagle dogs: Radiographic observations. *J. Korean Acad. Prosthodont.* **2013**, *51*, 307–314. [[CrossRef](#)]
32. Huh, J.B.; Lee, J.Y.; Lee, K.L.; Kim, S.E.; Yun, M.J.; Sim, J.S.; Shim, J.S.; Shin, S.W. Effects of the immobilization of heparin and rhPDGF-BB to titanium surfaces for the enhancement of osteoblastic functions and anti-inflammation. *J. Adv. Prosthodont.* **2011**, *3*, 152–160. [[CrossRef](#)] [[PubMed](#)]
33. Choo, T.; Marino, V.; Bartold, P.M. Effect of PDGF-BB and beta-tricalcium phosphate ( $\beta$ -TCP) on bone formation around dental implants: A pilot study in sheep. *Clin. Oral Implants Res.* **2013**, *24*, 158–166. [[CrossRef](#)] [[PubMed](#)]
34. Huh, J.B.; Park, C.K.; Kim, S.E.; Shim, K.M.; Choi, K.H.; Kim, S.J.; Sim, J.S.; Shin, S.W. Alveolar ridge augmentation using anodized implants coated with Escherichia coli-derived recombinant human bone morphogenetic protein 2. *Oral Surg. Oral Med. Oral Pathol. Oral Radiol. Endod.* **2011**, *112*, 42–49. [[CrossRef](#)] [[PubMed](#)]
35. Huh, J.B.; Kim, S.E.; Kim, H.E.; Kang, S.S.; Choi, K.H.; Jeong, C.M.; Lee, J.Y.; Shin, S.W. Effects of anodized implants coated with Escherichia coli-derived rhBMP-2 in beagle dogs. *Int. J. Oral Maxillofac. Surg.* **2012**, *41*, 1577–1584. [[CrossRef](#)] [[PubMed](#)]
36. Kim, S.E.; Kim, C.S.; Yun, Y.P.; Yang, D.H.; Park, K.S.; Kim, S.E.; Jeong, C.M.; Huh, J.B. Improving osteoblast functions and bone formation upon BMP-2 immobilization on titanium modified with heparin. *Carbohydr. Polym.* **2014**, *114*, 123–132. [[CrossRef](#)] [[PubMed](#)]
37. Jung, R.E.; Windisch, S.I.; Eggenschwiler, A.M.; Thoma, D.S.; Weber, F.E.; Hämmerle, C.H. A randomized-controlled clinical trial evaluating clinical and radiological outcomes after 3 and 5 years of dental implants placed in bone regenerated by means of GBR techniques with or without the addition of BMP-2. *Clin. Oral Implants Res.* **2009**, *20*, 660–666. [[CrossRef](#)] [[PubMed](#)]
38. Jung, R.E.; Glauser, R.; Schärer, P.; Hämmerle, C.H.; Sailer, H.F.; Weber, F.E. Effect of rhBMP-2 on guided bone regeneration in humans. *Clin. Oral Implants Res.* **2003**, *14*, 556–568. [[CrossRef](#)] [[PubMed](#)]



39. Boyne, P.J.; Lilly, L.C.; Marx, R.E.; Moy, P.K.; Nevins, M.; Spagnoli, D.B.; Triplett, R.G. De novo bone induction by recombinant human bone morphogenetic protein-2 (rhBMP-2) in maxillary sinus floor augmentation. *J. Oral Maxillofac. Surg.* **2005**, *63*, 1693–1707. [[CrossRef](#)] [[PubMed](#)]
40. Zhao, B.; Katagiri, T.; Toyoda, H.; Takada, T.; Yanai, T.; Fukuda, T.; Chung, U.I.; Koike, T.; Takaoka, K.; Kamijo, R. Heparin potentiates the in vivo ectopic bone formation induced by bone morphogenetic protein-2. *J. Biol. Chem.* **2006**, *281*, 23246–23253. [[CrossRef](#)] [[PubMed](#)]
41. Ho, Y.C.; Mi, F.L.; Sung, H.W.; Kuo, P.L. Heparin-functionalized chitosanealginate scaffolds for controlled release of growth factor. *Int. J. Pharm.* **2009**, *376*, 69–75. [[CrossRef](#)] [[PubMed](#)]
42. Lin, H.; Zhao, Y.; Sun, W.; Chen, B.; Zhang, J.; Zhao, W.; Xiao, Z.; Dai, J. The effect of crosslinking heparin to demineralized bone matrix on mechanical strength and specific binding to human bone morphogenetic protein-2. *Biomaterials* **2008**, *29*, 1189–1197. [[CrossRef](#)] [[PubMed](#)]
43. Le Guéhennec, L.; Soueidan, A.; Layrolle, P.; Amouriq, Y. Surface treatments of titanium dental implants for rapid osseointegration. *Dent. Mater.* **2007**, *23*, 844–854. [[CrossRef](#)] [[PubMed](#)]
44. Zhoua, D.; Ito, Y. Inorganic material surfaces made bioactive by immobilizing growth factors for hard tissue engineering. *RSC Adv.* **2013**, *3*, 11095–11106. [[CrossRef](#)]
45. Kim, S.E.; Song, S.H.; Yun, Y.P.; Choi, B.J.; Kwon, I.K.; Bae, M.S.; Moon, H.J.; Kwon, Y.D. The effect of immobilization of heparin and bone morphogenetic protein-2 (BMP-2) to titanium surfaces on inflammation and osteoblast function. *Biomaterials* **2011**, *32*, 366–373. [[CrossRef](#)] [[PubMed](#)]
46. Hong, S.; Kim, K.Y.; Wook, H.J.; Park, S.Y.; Lee, K.D.; Lee, D.Y.; Lee, H. Attenuation of the in vivo toxicity of biomaterials by polydopamine surface modification. *Nanomedicine (London)* **2011**, *6*, 793–801. [[CrossRef](#)] [[PubMed](#)]
47. Lee, H.; Dellatore, S.M.; Miller, W.M.; Messersmith, P.B. Mussel-inspired surface chemistry for multifunctional coatings. *Science* **2007**, *318*, 426–430. [[CrossRef](#)] [[PubMed](#)]
48. Fan, X.; Lin, L.; Dalsin, J.L.; Messersmith, P.B. Biomimetic anchor for surface-initiated polymerization from metal substrates. *J. Am. Chem. Soc.* **2005**, *127*, 15843–15847. [[CrossRef](#)] [[PubMed](#)]
49. Lee, D.W.; Yun, Y.P.; Park, K.; Kim, S.E. Gentamicin and bone morphogenetic protein-2 (BMP-2)-delivering heparinized-titanium implant with enhanced antibacterial activity and osseointegration. *Bone* **2012**, *50*, 974–982. [[CrossRef](#)] [[PubMed](#)]
50. Chaudhary, L.R.; Hofmeister, A.M.; Hruska, K.A. Differential growth factor control of bone formation through osteoprogenitor differentiation. *Bone* **2004**, *34*, 402–411. [[CrossRef](#)] [[PubMed](#)]
51. Zhang, Y.; Shi, B.; Li, C.; Wang, Y.; Chen, Y.; Zhang, W.; Luo, T.; Cheng, X. The synergetic bone-forming effects of combinations of growth factors expressed by adenovirus vectors on chitosan/collagen scaffolds. *J. Control. Release* **2009**, *136*, 172–178. [[CrossRef](#)] [[PubMed](#)]
52. Kim, N.H.; Lee, S.H.; Ryu, J.J.; Choi, K.H.; Huh, J.B. Effects of rhBMP-2 on sandblasted and acid etched titanium implant surfaces on bone regeneration and osseointegration: Spilt-mouth designed pilot study. *Biomed. Res. Int.* **2015**, *2015*, 1–11. [[CrossRef](#)] [[PubMed](#)]
53. Shi, Z.; Neoh, K.G.; Kang, E.T.; Poh, C.K.; Wang, W. Surface functionalization of titanium with carboxymethyl chitosan and immobilized bone morphogenetic protein-2 for enhanced osseointegration. *Biomacromolecules* **2009**, *10*, 1603–1611. [[CrossRef](#)] [[PubMed](#)]
54. Turksen, K.; Bhargava, U.; Moe, H.K.; Aubin, J.E. Isolation of monoclonal antibodies recognizing rat bone-associated molecules in vitro and in vivo. *J. Histochem. Cytochem.* **1992**, *40*, 1339–1352. [[CrossRef](#)] [[PubMed](#)]
55. Van den Beucken, J.J.; Walboomers, X.F.; Boerman, O.C.; Vos, M.R.; Sommerdijk, N.A.; Hayakawa, T.; Fukushima, T.; Okahata, Y.; Nolte, R.J.; Jansen, J.A. Functionalization of multilayered DNA-coatings with bone morphogenetic protein 2. *J. Control. Release* **2006**, *113*, 63–72. [[CrossRef](#)] [[PubMed](#)]
56. Skodje, A.; Idris, S.B.M.; Sun, Y.; Bartaula, S.; Mustafa, K.; Finne-Wistrand, A.; Wik, U.M.E.; Leknes, K.N. Biodegradable polymer scaffolds loaded with low-dose BMP-2 stimulate periodontal ligament cell differentiation. *J. Biomed. Mater. Res. A* **2015**, *103*, 1991–1998. [[CrossRef](#)] [[PubMed](#)]

